Efficiency Improvement of Solar Panels Through Parasitic Parameters Extraction and Maximum Power Improvement with Enhanced Slime Mold Optimization Under Partial Shading Conditions

S. venkateshwarlu
CVR College of Engineering
J V G Rama Rao (jvgramarao2@gmail.com)
BVC Institute of Technology and Science
Shaik Abdul Saleem
University of technology and Applied Sciences, Sulthanate of Oman

Research Article

Keywords: Maximum Power Point Tracking (MPPT), Triple Diode Model (TDM), Objective function, Penalty factor, Artificial Bee Swarm Optimization (ABSO)

Posted Date: April 25th, 2023

DOI: https://doi.org/10.21203/rs.3.rs-2851161/v1

Additional Declarations: No competing interests reported.

Efficiency Improvement of Solar Panels Through Parasitic Parameters Extraction and Maximum Power Improvement with Enhanced Slime Mold Optimization Under Partial Shading Conditions

S. venkateshwarlu[1], J V G Rama Rao[2*], Shaik Abdul Saleem[3]

[1]Department of Electrical Engineering, CVR College of Engineering, Ibrahimpatnam-501510, India.
[2]Department of Electrical and Electronics Engineering, BVC Institute of Technology and Science, Amalapuram, AP- 533221, India
[3]University of technology and Applied Sciences, Suhar, Sulthanate of Oman- 133, India

[*]**Corresponding Author:** J V G Rama Rao (jvgramarao2@gmail.com)

Abstract: Solar energy offers several environmental, economic, and energy security advantages. Parasitic parameters and shading on solar panels can reduce efficiency. This paper presents a bio-inspired Enhanced Slime Mold (ESM) algorithm search strategy to find the optimal power point by simulating the behaviour of slime molds in a virtual environment. In a solar panel, proposed ESM provides not only for parameter extraction but also serves as Maximum Power Point Tracking (MPPT) during Partial Shading Conditions (PSC). Proposed ESM dynamic behaviour is examined under solar irradiation and various temperature conditions. The effectiveness of proposed technique has been validated by extracting parameters from conventional polycrystalline and monocrystalline modules in the form of a 5S-5P arrangement. In the instance of MPPT operation, the proposed ESM algorithm is compared with Ant Bee Colony and Perturb& Observe (ABC-PO) to determine its efficacy. Moreover, during extraction of unknown parameters of solar cell ESM is compared with existing optimization algorithms such as Artificial Bee Swarm Optimization (ABC SO), Genetic Algorithm (GA), Covariant Matrix (CM), Ant Bee Colony (ABC), and Advanced Particle Swarm Optimization (APSO). In this connection, proposed ESM algorithm is superior to above-mentioned algorithms due to high accuracy, a smaller number of computations, and minimum computational time.

Keywords: Maximum Power Point Tracking (MPPT), Triple Diode Model (TDM), Objective function, Penalty factor, Artificial Bee Swarm Optimization (ABSO)

1. Introduction

Solar energy is rapidly gaining popularity worldwide as an affordable, clean, and renewable source of energy. The International Energy Agency (IEA) has projected that solar energy will become the largest source of electricity in the world by 2050, accounting for almost one-third of global electricity production [1]. As of 2021, the installed solar energy capacity worldwide is over 770 GW, with an additional 170 GW expected to be added in 2022 alone [2]. The global solar energy market has been driven by declining solar panel costs, supportive government policies, and the need to address climate change. In recent years, countries like China, the United States, and India have emerged as major solar energy producers. According to a report by the Solar Energy Industries Association (SEIA), the United States added 15.9 GW of solar energy capacity in 2020, while China added 48.2 GW. while India stands 4th globally in Renewable Energy Installed Capacity, 4th in Wind Power capacity & 4th in Solar Power capacity (as per REN21 Renewables 2022 Global Status Report) [3],[4].

Direct current is produced by a solar cell when it is exposed to sunlight. Photovoltaic (PV) modules low conversion efficiency can be attributed to the nonlinear characteristics of solar cells. So, it is essential to utilize all the energy generated by the PV cells. Also, the maximum power produced by a PV module varies based on elements including temperature, irradiance level, dirt, and the installation requirements, such as the local geography and climate [5]. It is vital to research issues related to precise weather forecasting because solar energy happens naturally and without expense to humanity. Both grid-connected and off-grid generators can use PV systems. These units provide electricity to places that lack access to or have subpar grid power. It has been discovered that the solar cell's Power-Voltage (P-V) characteristics change depending on the atmosphere in the area (i.e., solar insolation and temperature). At that time, the cell's output is at its maximum [6].

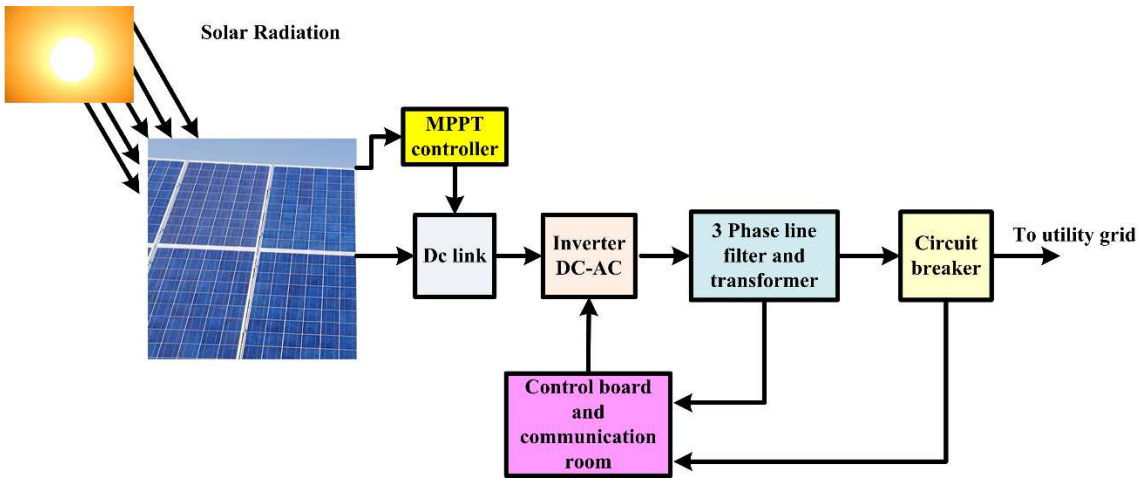

Fig. 1 Standard PV system for utility grid.

Based on considering how quickly they can monitor maximum output under partial shading circumstances, the amount it will cost to implement, how difficult it is, and other factors. The three main types of these meta-heuristic MPPT algorithms are differential evaluation, swarm intelligence (SI), and bio-inspired (BI) (DE). SI contains the following algorithms: slap swarm algorithm (SSA), emperor penguin optimization (EPO), cat swarm optimization (CSO), whale optimization (WOA), Gray Wolf Optimisation (GWO), artificial bee colony (ABC), particle swarm optimisation (PSO), and Jaya algorithm (JA). Cuckoo search (CSA), moth flame optimisation (MFO), bat search algorithm (BA), grasshopper optimisation (GOA), and the firefly method (FFA) are examples of approaches used in business intelligence (BI). Genetic algorithms and differential evolution (DE) are both being studied in relation to EC approaches (GA) [7]-[9]. In [10] proposed fuzzy adaptive differential evolution algorithm for identification of PV module parameters. While improving convergence parameter adjustment strategy is constructed to improve the local search capability of PV module.

The unknown parameters extraction is essential for obtaining better performance of PV panels. Coyote Optimization is helpful to extract unknown parameters and estimated parameters in an accurate manner [11]. Various solar panels such as single-diode, double-diode, and triple-diode models have eliminated parameters. The extraction is based on P-V and I-V characteristic data. Sairaj *et al.,* [12] proposed a Tabu search optimization for eliminating the parasitic or unknown parameters from PV modules such as polycrystalline, monocrystalline, and thin film. The Enhanced Slime Mold (ESM) optimization algorithm addresses solar panel modelling and tracking behaviour. The conventional grid integrated PV system is shown in Figure 1. This paper mainly contributes the performance of PV panel under various insolation levels and temperature regions. Structure-wise, this article goes as follows: Partial shading and changes in the I-V and P-V curves of a solar cell were explored together with their corresponding circuit models in Section 2. In section 3, the implementation of the suggested SM MPPT algorithm as well as its results are compared with that of ABC-PSO. The simulation results of proposed ESM algorithm are presented in Section 4. Finally, the conclusion is provided in section 5.

2. Modelling of solar cell

2.1. Single diode model

The photo generated current is parallelized using the current source from the Single Diode Model (SDM) solar cell, and the diode acts as the half-wave rectifier. The model is easy to implement, but required information is not available from SDM [13]. Figure 2 depicts the design of SDM PV cell. In SDM involves photo generated current (I_{Ph}), while shunt resistance (R_{Sh}) represents the PN junction leakage current and is in parallel with diode, diode current (I_D), series resistance (R_S) reflects about the resistance of surface of electrode, V_0 is obtained in the form of output voltage. Therefore, from Figure 2, according to Kirchhoff's current law, the output current (I_0) is represented as

$$I_0 = I_{ph} - I_d - I_{sh} \tag{1}$$

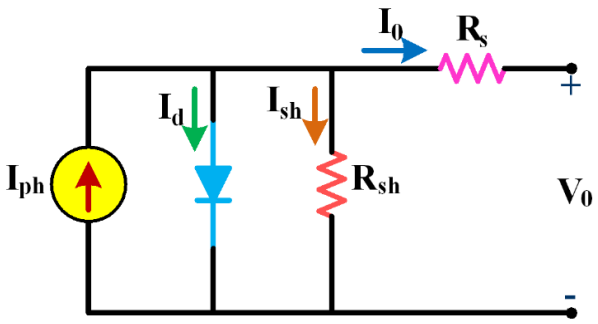

Fig. 2 Equivalent circuit for SDM solar cell.

The diode current (I_D) equation is based on Shockley equation computed as

$$I_D = I_{rs}\left[\exp\left(\frac{q(V_0 + IR_S}{n \cdot k \cdot T}\right) - 1\right] \tag{2}$$

Where I_{rs} is the reverse saturation current, n is the ideality factor, k is the Boltzmann's constant i.e., 1.380×10^{-23} J/K, q denotes the charge of an electron (1.602×10^{-19} C) and T denotes the cell absolute temperature. The shunt resistance current (I_{Sh}) is calculated as

$$I_{Sh} = \frac{V + I \cdot R_S}{R_{Sh}} \tag{3}$$

By substituting Eq. (2) and Eq. (3) into Eq. (1), the solar cell output current is represented as

$$I_0 = I_{ph} - I_{rs}\left[\exp\left(\frac{q(V + I \cdot R_S)}{n \cdot k \cdot T}\right) - 1\right] - \frac{V + I \cdot R_S}{R_{Sh}} \tag{4}$$

2.2. Double diode model

The Double Diode Model (DDM) consists of seven unknown parameters, i.e., Photocurrent (I^l_{Ph}), diffusion current (I_{rs1}), reverse saturation current (I_{rs2}), penalty factors (n_1 and n_2), R_s and R_{Sh}. Figure 3 depicts the equivalent circuit of DDM solar cell [14]. The output current equation is calculated using Eq. (5).

$$I_0 = I_{ph} - I_{rs1}[\alpha_1] - I_{rs2}[\alpha_2] - \frac{V_0 + I_0 \cdot R_S}{R_{Sh}} \tag{5}$$

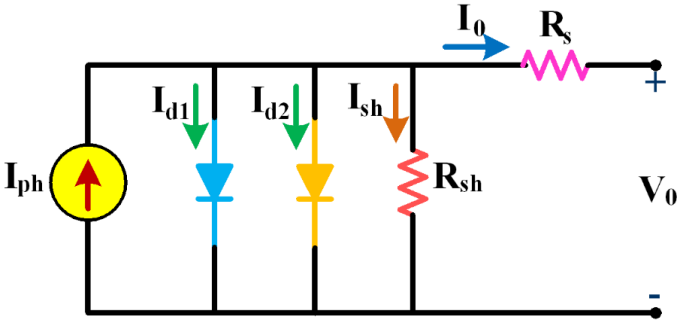

Fig. 3 Equivalent circuit for DDM solar cell.

2.3. Three diode model

Including the effects of leakage currents and grain boundaries in PV models using the TDM is suggested for enhancing overall accuracy [15]. The configuration of TDM is same as DDM except for the third shunted diode. The schematic of TDM is depicted in Figure 4.

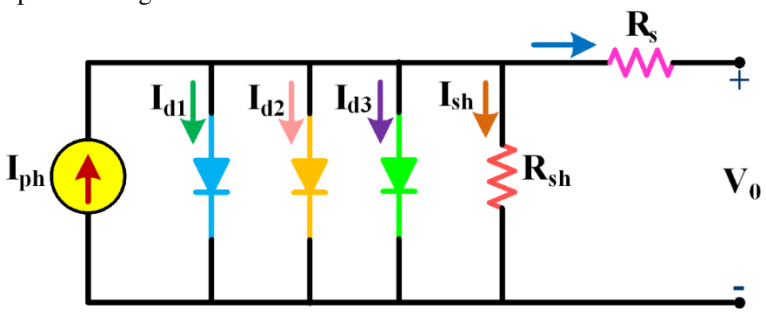

Fig.4 Equivalent circuit for TDM solar cell.

$$I_L = I_{ph} - I_{d1} - I_{d2} - I_{d3} - I_{sh} \tag{7}$$

$$I_0 = I^I{}_{Ph} - I_{rs1}[\alpha_1] - I_{rs2}[\alpha_2] - I_{rs2}[\alpha_3] - \frac{V_0 + I_0 \cdot R_S}{R_{Sh}} \tag{8}$$

$$\left.\begin{aligned} \alpha_1 &= \exp\left(\frac{q(V_0 + I_0 \cdot R_S)}{n_1 \cdot k \cdot T}\right) - 1 \\ \alpha_2 &= \exp\left(\frac{q(V_0 + I_0 \cdot R_S)}{n_2 \cdot k \cdot T}\right) - 1 \\ \alpha_3 &= \exp\left(\frac{q(V_0 + I_0 \cdot R_S)}{n_3 \cdot k \cdot T}\right) - 1 \end{aligned}\right\} \tag{9}$$

The parameter extraction issue is solved by employing the objective function (J^I), and the halting criteria is readily met as a result. The root-mean-square Error (RMSE) is used to help define the objective function. RMSE defines J^I, which in turn is applied to proposed SM Technique. Therefore, the extraction of data is identified in a quick manner. RMSE is formulated as

$$RMSE = \sqrt{\frac{1}{N^I}\sum_{i=1}^{N^I} F(V_E, I_E, \lambda)^2} \tag{10}$$

Where, F (V_E, I_E, λ) is the error function, V_E, I_E is the experimental values of voltage and current. The difference between experimental and estimated values is calculated. N^I denotes the data set of parasitic parameters, and λ denotes the undetermined vector parasitic parameters. such as for SDM λ is (I_{Ph}, I_d, n, R_s, and R_{sh}), for DDM the λ is (I_{Ph}, I_{rs1}, I_{rs2}, n_1, n_2, R_s, and R_{sh}) and in TDM the parasitic parameters are (I_{Ph}, I_{sd1}, I_{sd2}, I_{sd3}, n_1, n_2, n_3, R_s, and R_{sh}). The convergence pattern of SDM, DDM, and TDM are shown in Figure 5 for 500 iterations.

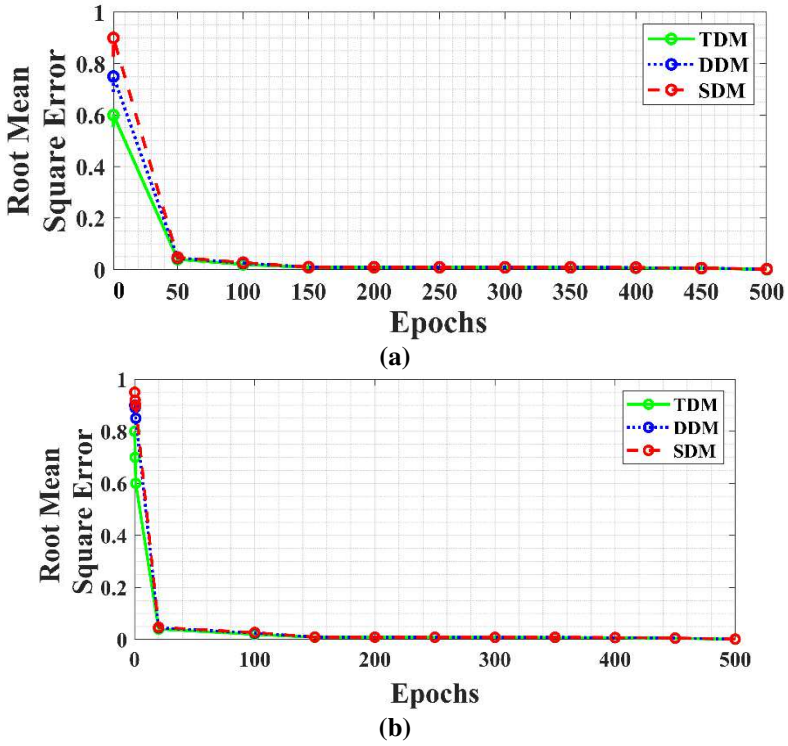

Fig.5 RMSE convergence trends for solar cells and PV modules under consideration using the proposed ESM method -based models: (a) Monocrystalline (STP250S), (b) Polycrystalline (SPR-P5-220UPP).

The parameters of a solar panel depend on several factors, including the type of solar cell technology used, the size of the panel, and the operating conditions. The common parameters of solar panels are Maximum Power (P_{max}), Voltage at maximum Power (V_{MP}), Open Circuit Voltage (V_{OC}), Short Circuit Current (I_{SC}), Cell Efficiency (%), and Operating temperature. The electrical parameters of monocrystalline and polycrystalline solar panels are represented in Table 1.

Table 1 Electrical parameters of solar cell

Parameters	Monocrystalline (STP250S)	Polycrystalline (SPR-P5-220UPP)
Maximum Output Power (P_{max})	250W	250W
Voltage at Maximum Power (V_{MP})	29.63V	27.97V
Current at maximum Power (I_{MP})	7.18A	9.26A
Open Circuit Voltage (V_{OC})	32.01V	29.7V
Short Circuit Current (I_{SC})	8.07A	8.12A
Cell Efficiency (%)	22.89	16-18%
Operating Temperature	-40°C to +85°C	-40°C to +85°C

2.4. Effect of environmental factors on solar cell

2.4.1. Effect of temperature variations

There is a direct relationship between temperature and solar cell efficiency. Figures 6(a) and 7(a) depict P-V and I-V curves of monocrystalline and polycrystalline solar cells. These solar cells said characteristics are analyzed under 45^0C,25^0C and 10^0C and it clearly shows that when the temperature on solar cells increases the open circuit voltage falls in both monocrystalline and polycrystalline but there is drastic change in polycrystalline solar cell P-V & I-V curves [16].

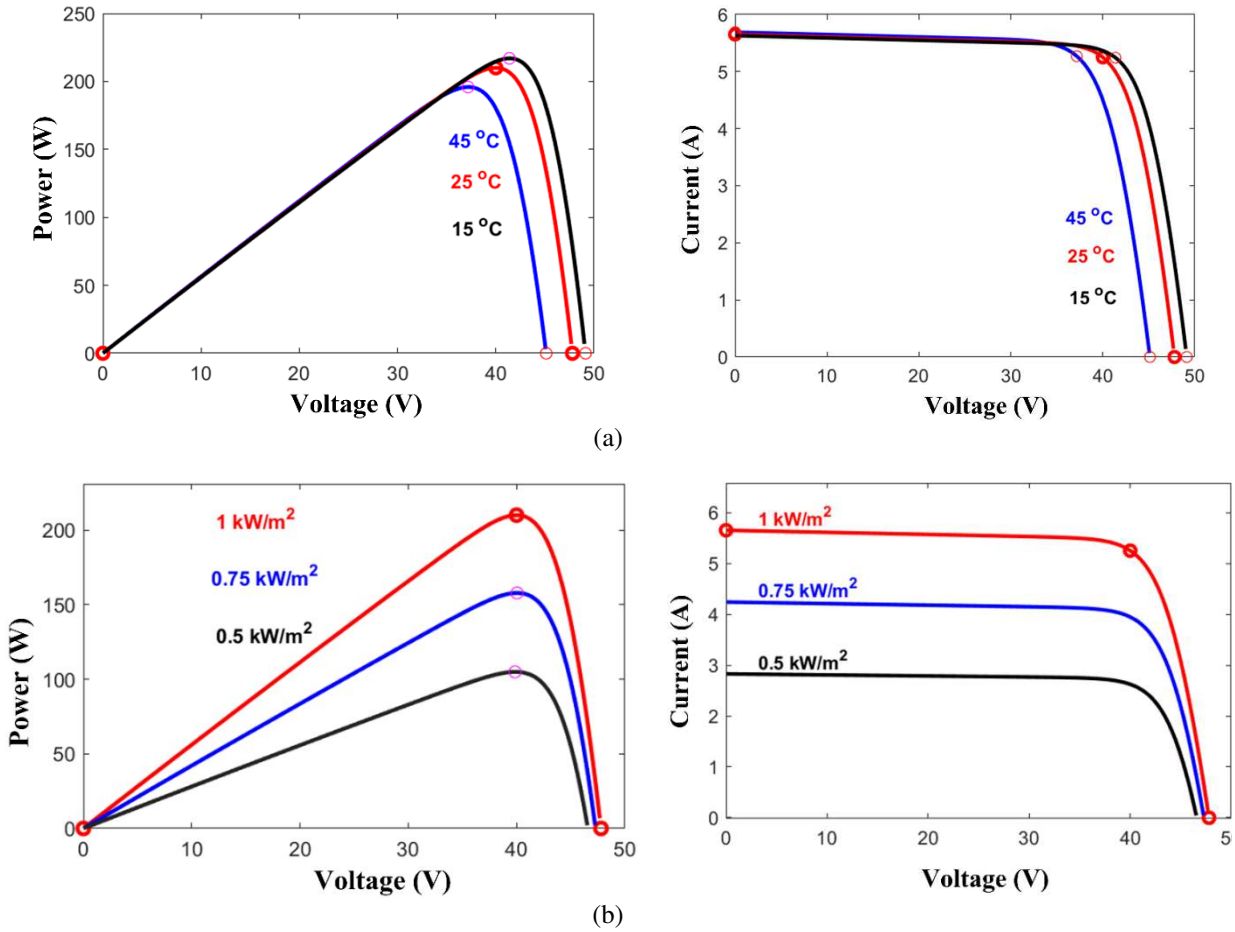

Fig.6 P-V and I-V characteristics of (a) Monocrystalline (b) Polycrystalline solar cell.

2.4.2. Effect of insolation variations

Here we have analyzed P-V & I-V characteristics with 1000,750 and 500 insolation levels. Figures 6(b) and 7(b) are clearly showing that when the insolation level rises the short circuit current will increase correspondingly. and if the level of insolation is fallen the maximum power point will be decreasing in both monocrystalline and polycrystalline cells. and it is evidenced that polycrystalline solar cell's short circuit and maximum power point is drastically changing compared to monocrystalline solar cells under similar insolation variations [17].

2.5. Partial shading conditions

Partial-Shadow State to put it simply, partial shadowing is a common problem for photovoltaic systems. Any obstruction that partially blocks the sun's rays from reaching surfaces (like a PV panel) produces an image known as a shadow on that surface (PSC). Therefore, constant uniform irradiance is impossible due to weather variations such as clouds, rain, storms, etc. Not only can trees and buildings cast shadows, but they cast several kinds of shadows. Therefore, due to this effect, a series-connected solar array cannot receive the same amount of incident irradiance [18]. The output power generation of the Photovoltaic modules drops because of shade on the PV array. Figure 8(a) and 8(b) clearly shows that Various local peaks (LMPPs) on the P-V curve can be attributed to the Photovoltaic module's nonlinear output I-V characteristics. As a result, hotspots result from shadowing, severely damaging these cells.

Major disadvantages of shading include current imbalance within a Photovoltaic string & voltage imbalance between parallel modules. Variables such as PV string configuration, module type, bypass diode location, different shading patterns, and shading intensity all contribute to the overall magnitude of the effect of shade [19]. When another partially covers one cell, the current through that cell is reduced relative to the other cells in the string. To compensate, more electricity will flow through the exposed cells. This causes the cell to behave as a reverse diode.

As a result, the darkened cell restricts the amount of electricity that may travel along the string. Therefore, the PV string's output power decreases. It is important to note that the drop in output power produced by the PV string is more noticeable as the number of partial shadings rises. As the percentage of shaded modules rises, the P-V curve becomes more complex, with the number of peaks. The shading effect can be reduced by adding a bypass diode across a series-connected string of specific cells.

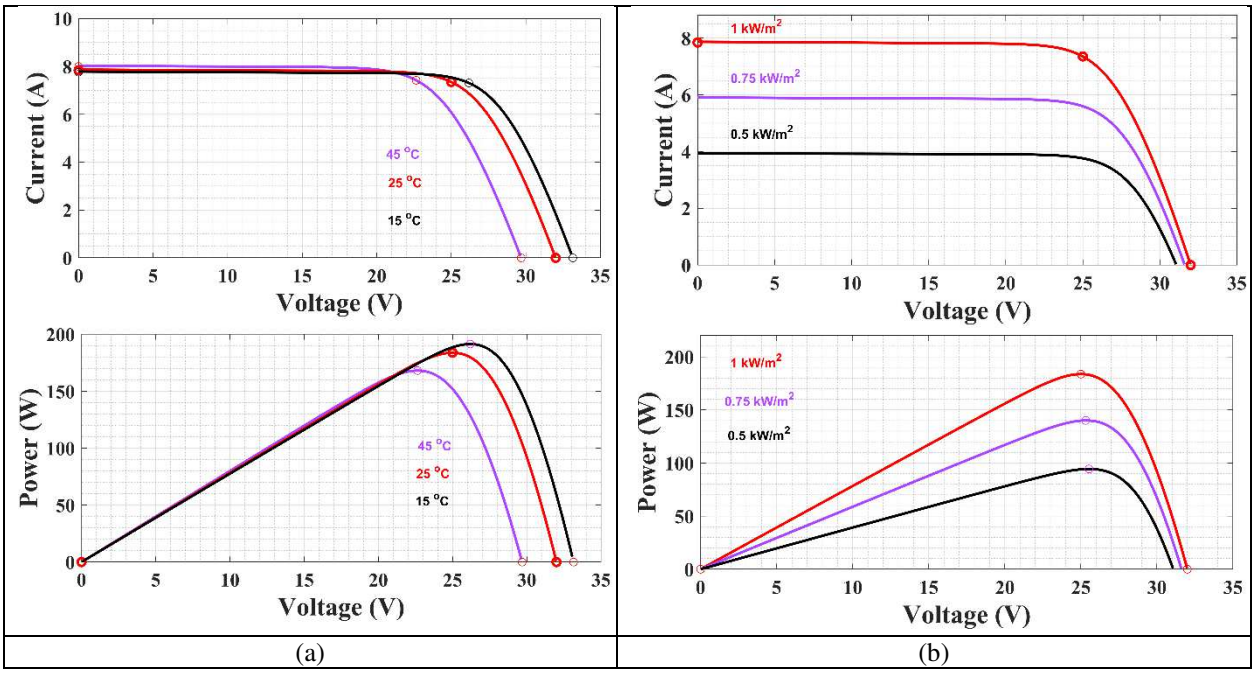

Fig.7 P-V and I-V characteristics of (a) Monocrystalline (b) Polycrystalline solar cell.

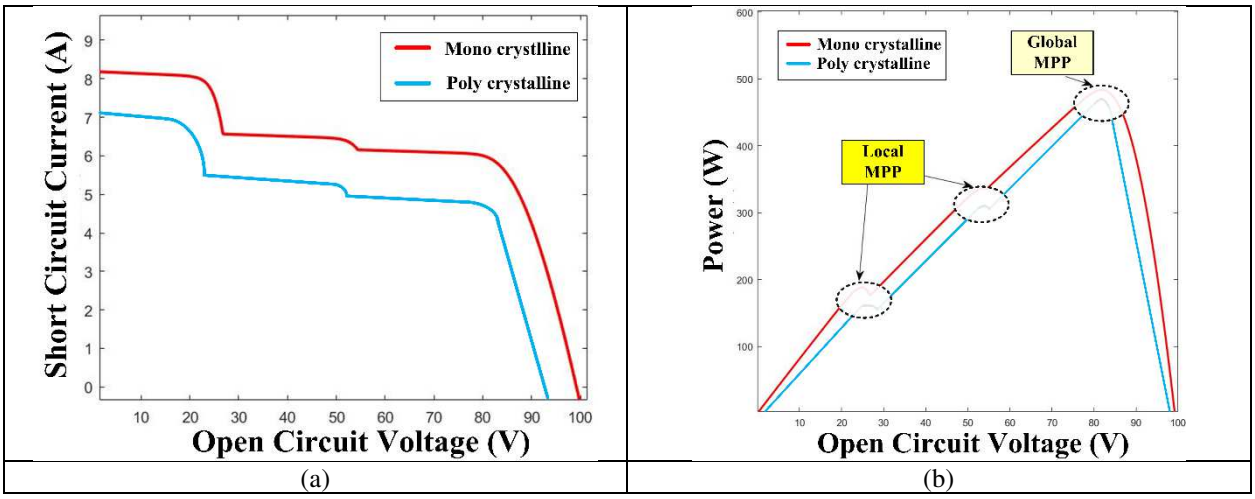

Fig.8 Monocrystalline and polycrystalline solar panel (a) I-V Curve, (b) P-V Curve.

3. Proposed Enhanced Slime Mold algorithm

In recent years, a novel technique has emerged that utilizes the behavior of slime molds to optimize the power output of solar panels. ESM inspired by the behavior of slime molds, which exhibit a unique ability to find the shortest path between two points. Researchers studying the behavior of SM, they were able to create an algorithm that could solve optimization problems in a similar manner.

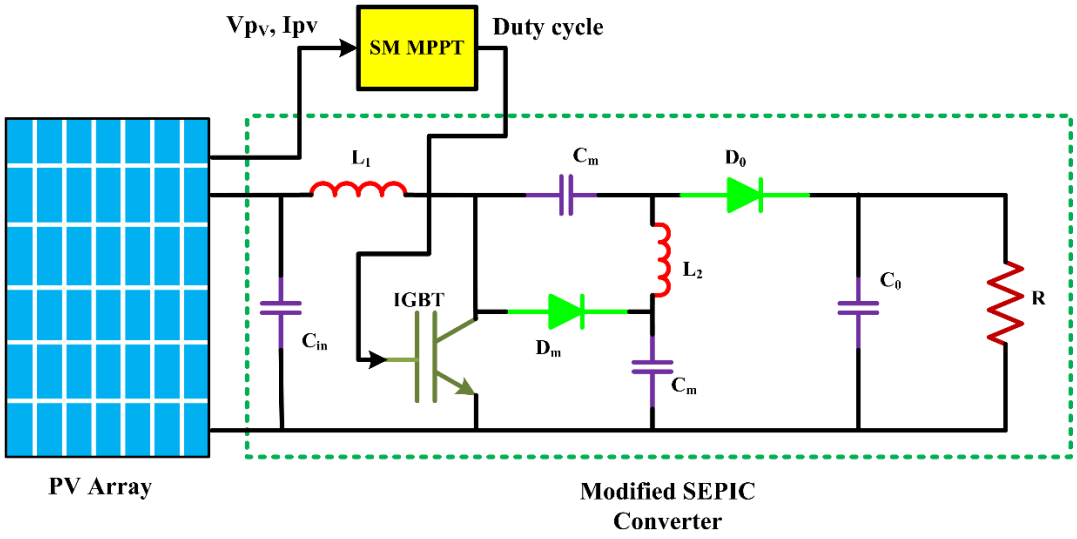

Fig. 9 Proposed ESM used in PV array.

Proposed ESM technique takes inspiration from the way SM seeks out food sources. SM grows in a pattern of branching tubes, and when it encounters a food source, it reorganizes its tubes to create the most efficient network for transporting nutrients. In case of MPPT technique, the solar panel is represented as a food source, and the MPPT algorithm mimics the behavior of SM to find the optimal path to the maximum power point. The algorithm creates a network of tubes that represent the different voltage levels of the solar panel, and the SM-like process determines the most efficient path to the maximum power point by finding the path with the least resistance [20]. The advantage of ESM technique is that it can handle non-linear and non-convex power-voltage curves, which are often found in real-world solar panels. Additionally, this technique is computationally efficient and can converge to the maximum power point quickly. ESM MPPT technique is a promising optimization technique for solar power systems as represented in Figure 9.

3.1. The Quest for Food

The following mathematical formulation can be used to describe and explain the slime mould convergence pattern.

$$X^{I}(t+1)=\begin{cases} X_{b}^{I}\times vb\times(W\times X_{A}^{I}(t)-X_{B}^{I}(t)), r<p \\ vc\times X^{I}(t), r\geq p \end{cases} \tag{11}$$

where $X^{I}(t)$ is current position of SM, vb and vc are random numbers between [a, -a] & [-1,1], $X^{I}_{A}(t)$ and $X^{I}_{B}(t)$ are two random individuals, $X^{I}_{b}(t)$ is the optimal adaptation, t is current number of iterations, w is weight of coefficient, and p represents as

$$p=\tanh\left|S(i)-DF\right| \tag{12}$$

Where i is in the range $[1, n]$, $SI(i)$ is the adaption value of the lower i Mucor individuals, and DF is the population member with the best adaptation.

$$a=\arctan h(-(\frac{t}{T})+1) \tag{13}$$

$$W(SI(i)) = \begin{cases} 1 + r \times \log\left(\dfrac{bF - S(i)}{bF - wF} + 1\right), \Pr \\ 1 - r \times \log\left(\dfrac{bF - S(i)}{bF - wF} + 1\right), Ot \end{cases} \quad (14)$$

$$SI = sort(S) \quad (15)$$

where Pr represents the first half of the individual rank, Ot represents the leftover individuals, r is a random number among [0,1], wF represents the worst fitness value, bF represents the best fitness value for the latest number of iterations, and SI (i) represents the fitness sequence, which denotes the increasing series.

3.2. Food Wrapping

An example of the formula used to monitor the movement of every slime mould is as follows:

$$X^I(t+1) = \begin{cases} rand \times (uB - LB) + LB, rand < z \\ X_b^I \times vb \times (W \times X_A^I(t) - X_B^I(t)), r < p \\ vc \times X^I(t), r \geq p \end{cases} \quad (16)$$

where z is the restricted value (0.03), rand is a random number among [0, 1], and UB and LB are the higher and lower bounds of the current iteration count, respectively.

3.3. Obtaining Food

The amount of *vc* fluctuates between [-1, 1], and the value of *vb* is randomly picked between [-a, a], finally convergent to 0. The following is the formula:

$$vc = [-b, b] \quad (17)$$

$$b = 1 - \frac{b}{T} \quad (18)$$

After first extracting the parasitic parameters from SDM, DDM, and TDM solar panels, the proposed ESM optimisation algorithm then performs MPPT by continually changing the operating point of the solar panel to maintain it at the MPP under PSC conditions. The process flow of proposed ESM is depicted in Figure 10.

3.1. Modified SEPIC converter

Most of the research in residential applications is concentrated on module-integrated converters, which transport energy produced by one Photovoltaic module to the grid via a dedicated converter incorporated with the PV module. The modularity of this PV production system allows for easy expansion of installed power, individual MPPT, and mitigation of partial shadowing and panel imbalance effects, all of which improve energy collecting capability. Yet, there are significant design issues in an ac module construction, such as increasing efficiency, lowering costs, and ensuring dependable functioning over the module's lifetime. Because of the low input voltage, high input current, high output voltage, and static gain of the dc-dc converter, high efficiency operating is a difficulty [21]. The static gain of the proposed converter is higher than the obtained with the classical boost is represented as

$$\frac{V_0}{V_i} = \frac{1 + D}{1 - D} \quad (19)$$

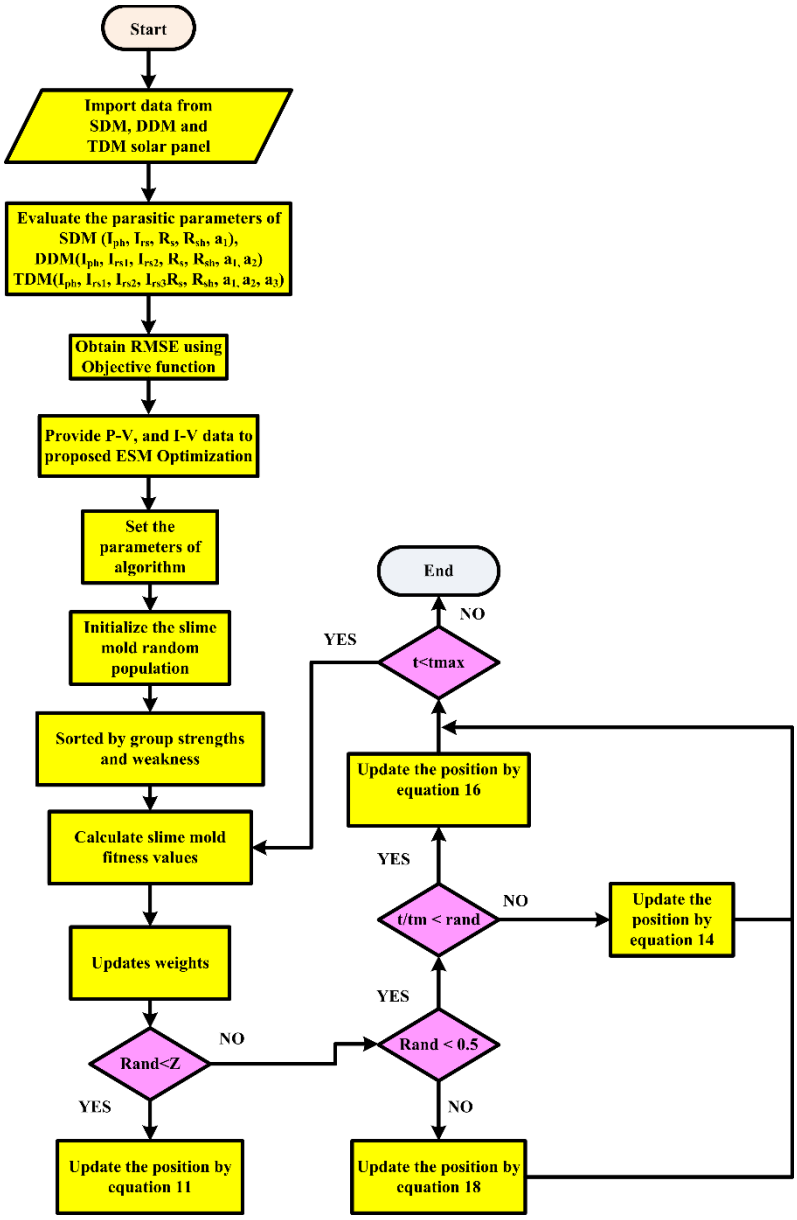

Fig.10 Flow chart of Proposed SM optimization algorithm.

The maximum switch voltage is equal to the VCM voltage. Therefore, the switch voltage will be lower than the converter output voltage is obtained as

$$\frac{V_{CM}}{V_i} = \frac{1}{1-D} \tag{20}$$

The voltage across the Cs capacitor is calculated by (3)

$$\frac{V_{CS}}{V_i} = \frac{D}{1-D} \tag{21}$$

However, the static gain, as well as the CM & CS capacitor voltages operated in DCM, are shown in (22), (23), & (24), respectively.

$$\frac{V_0}{V_i} = 1 + \frac{V_i \cdot D^2}{2 \cdot i_0 \cdot L_{eq} \cdot f} \tag{22}$$

$$\frac{V_{CM}}{V_i} = 1 + \frac{V_i \cdot D^2}{4 \cdot i_0 \cdot L_{eq} \cdot f} \tag{23}$$

$$\frac{V_{CS}}{V_i} = \frac{V_i \cdot D^2}{4 \cdot i_0 \cdot L_{eq} \cdot f} \tag{24}$$

where

$$L_{eq} = \frac{L_1 \cdot L_2}{L_1 + L_2} \tag{25}$$

Commercial monocrystalline and polycrystalline PV typically have a maximum output power (P_{MPP}) of less than 350W. Maximum power point voltage (V_{MPP}) ranges from 15 to 40V. P_{MPP} = 100 W with V_{MPP} = 15 V, P_{MPP} = 200 W with V_{MPP} = 30 V, and P_{MPP} = 300 W with V_{MPP} = 40 V are common specifications based on the number of photovoltaic cells. The specification P_{MPP} = 210 W with V_{MPP} = 40 V was used in this investigation, but raising the PV module power increases the voltage at the maximum power point. Under this circumstance, the dc-dc converter input current and conduction losses remain nearly constant. In this study, we have been using a Modified SEPIC converter for the implementation of ESM strategy . The typical option is to employ separate dc-dc converters whenever a large step-up ratio is required for the execution of the first power stage. We can raise the converter static gain by adjusting the transformer turns ratio.

The isolated approach, however, has certain drawbacks, including efficiency degradation brought on by power transformer losses & inherent variables such leakage inductance. The weight and volume of the converter are significantly influenced by the power transformer as well. Because of the high cost of power output, such as solar modules or fuel cells, power converters utilised with renewable energy sources must be very efficient. The converter power density is an important design consideration for embedded systems as well as portable devices. As a result, solutions that allow the power transformer to be removed can improve the system's efficiency and power density. The classical non-isolated dc dc-dc converters, on the other hand, have a finite step-up static gain ($q = V_o / V_i$). The boost converter, a classic non-isolated step-up dc-dc converter, normally performs with adequate both static and dynamic performances at a duty cycle close to D = 0.8, providing an output voltage four times the input voltage. A static gain of $q = 4$ is a limited value for the applications studied in this research.

4. Results and Discussions

The performance of the proposed ESM optimization algorithm is validated through approximation of model parameters of two PV cells which are Monocrystalline (DS-500M6-96), and Polycrystalline (SPR-P5-500-UPP) under various irradiance and temperature. Residual error is evaluated to attain accuracy in PV panel. The suggested ESM optimisation algorithm is controlled by the following parameters: maximum number of iterations, 500 iterations, and 500 slime moulds. The suggested ESM model is run on a MATLAB 2021a platform with an Intel(R) Core (TM) i5-8350U CPU at 1.70GHz and 16GB RAM. Figure 8 depicts RMSE convergence curves with respect to computational time. ABSO is the method that requires the most computing time due to its most intricate organisational structure. In contrast, the computational time required by other algorithms such as GA, CM, ABC, and APSO progressively decreases. The iteration time required by the proposed ESM method to calculate the parameters is the smallest possible amount as seen in Figure 11.

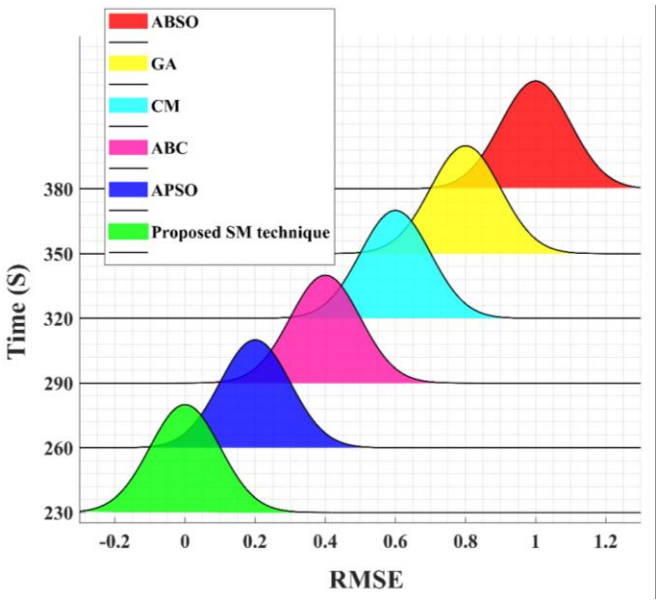

Fig.11 Convergence behaviour of proposed ESM algorithm.

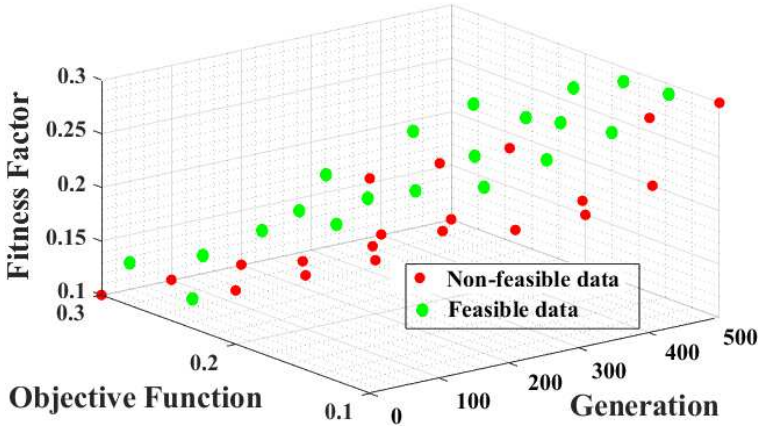

Fig.12. Feasible and Non-feasible data extraction.

The fitness factor decides the effectiveness of extraction process, so the much amount of feasibility is present in proposed ESM technique. The term feasibility means the parameters are easily managed towards the computation process without any complexity. Therefore, the convenient extraction process is obtained using proper computations. The non feasible parameters are filtered out initially during the data extraction process. Figure 12, depicts the feasible parameters are in green colour and non-feasible parameters are represented in red colour.

4.1. ESM for Parasitic parameter extraction

To know about the flexibility and accuracy of proposed ESM technique is represented in the form of union parameter. The convergence time is determined by the type of iterations executed for existing and proposed ESM technique. The time consumption for ABSO algorithm is more than proposed ESM technique, which represents the proposed algorithm has fast convergence operation as compared to other existing algorithms for optimum number of iterations. According to Table 2, the suggested ESM technique has the fewest iterations and takes the least amount of time for a 220W Polycrystalline SDM solar module (SPR-P5-250UPP), which is 314 seconds.

Because of the large number of iterations, the ABSO method takes 489 seconds to compute. Simulated data is used as a comparison for other existing techniques throughout the first execution process. The derived ABSO parameters are (0.774A, 0.64785A, 0.072479, 82.572, and 1.51), whereas the proposed ESM method values are (0.759A, 0.43197A, 0.048632, 84.235, and 1.44). As a result, when compared to other current algorithms, the suggested ESM technique has the best optimum performance levels. In the same way, Table 3 describes that simulated comparison of data for 220W Monocrystalline (STP250S) SDM PV module. The information retrieved from ABSO technique for the parameters IPh, Irs, RS, RSh, and n1 are 0.574A, 0.34791μA, 0.062519Ω, 92.143Ω, 1.51. The extracted parameter data obtained from proposed ESM algorithm are IPh (0.519A), Irs (0.33117μA), RS (0.049272Ω), RSh (74.548Ω), and a1 (295 sec) Observation shows that the pre-existing predicted values has substantially identical numerical values to the suggested ESM technique when compared to ABSO, GA, CM, ABC, & APSO.

Table 2 Estimated model parameters for SDM of (SPR-P5-250UPP) polycrystalline solar cell.

Algorithm	I_{Ph} (A)	I_{rs} (μA)	R_S (Ω)	R_{sh}(Ω)	a_1	Time (S)
ABSO [22]	0.774	0.64785	0.072479	82.572	1.51	489
GA [23]	0.770	0.59752	0.069624	76.329	1.48	446
CM [24]	0.768	0.53183	0.065379	78.914	1.47	398
ABC [25]	0.768	0.49529	0.058542	66.482	1.46	383
APSO [26]	0.760	0.47494	0.053632	92.752	1.45	367
Proposed ESM	0.759	0.43197	0.048632	84.235	1.44	314

Table 3 Estimated model parameters for SDM of (STP250S) Monocrystalline solar cell.

Algorithm	I_{Ph}	I_{rs} (μA)	R_S (Ω)	R_{sh}(Ω)	a_1	Time (S)
ABSO	0.574	0.34791	0.062519	92.143	1.51	452
GA	0.560	0.39753	0.059321	106.467	1.38	441
CM	0.558	0.38104	0.055874	68.652	1.37	381
ABC	0.542	0.37509	0.054327	76.124	1.36	373
APSO	0.530	0.36414	0.051432	82.542	1.55	342
Proposed ESM	0.519	0.33117	0.049272	74.548	1.34	295

The characteristics of 220W polycrystalline DDM solar panel are represented in Table 4. In ABSO algorithm and ESM algorithm the extracted parameters I_{Ph}, I_{rs1}, I_{rs2}, R_S, R_{Sh}, a_1, and a_2 are (0.764A, 0.44785μA, 0.5495μA, 0.0579Ω, 84.572Ω, 1.34, and 1.59), and (0.76A, 0.33197 μA, 0.5372μA, 0.0521Ω, 64.235Ω,1.38, and 1.62). According to the table, the suggested ESM technique has the shortest computation time, 324 seconds, when compared to other existing approaches such as ABSO (429 seconds), GA (416 seconds), CM (388 seconds), ABC (363 seconds), and APSO (357 sec). In ABSO technique huge computational time i.e., 412 sec is shown in Table 5. The remaining techniques are GA (404 seconds), CM (398 seconds), ABC (373 seconds), and APSO (373 seconds) (347 sec). As a result, it is important to keep in mind that the suggested ESM method has the shortest computational time, 317 seconds. ABSO method yielded the parasitic parameters (0.621A, 0.4587A, 0.4239A, 0.0287, 64.572, 1.24, and 1.49). The APSO approach is tied for second place. for eliminating extracted parameters and obtained numerical values are (0.592A, 0.34947μA, 0.4009μA, 0.0295Ω, 69.637Ω,1.24, and 1.32). Finally, the proposed ESM technique has preferable both in terms of effectiveness and parasitic quantitative data are 0.586A (I_{Ph}), 0.31196μA (I_{rs1}), 0.3974μA (I_{rs2}), 0.0277Ω (R_S), 61.715Ω (R_{Sh}), 1.21, and 1.32. Table 6 shows the retrieved parameters of a 220W TDM PV module. According to the table, the ABSO algorithm has a large computing time of 402 seconds.

The remaining strategies are GA (384 seconds), CM (368 seconds), ABC (343 seconds), & APSO (327 sec). As a result, it is noteworthy to note that the suggested ESM technique has the shortest computational time, which is 297 seconds. From the ABSO method, the parasitic factors I_{Ph}, I_{rs1}, I_{rs2}, I_{rs3}, R_S, R_{Sh}, a_1, a_2, & a_3 are (0.498A, 0.293A, 0.247A, 0.239A, 0.0143, 74.198, 1.94, 1.99, and 1.99). The proposed ESM approach performs well, with parasitic numerical values of 0.422A (I_{Ph}), 0.227A (I_{rs1}), 0.211A (I_{rs2}), 0.154A (I_{rs3}), 0.0099 (R_S), 51.115 (R_{Sh}), 1.91(a1), 1.92 (a2), and 1.91 (a3) (a3). In ABSO algorithm and ESM technique the extracted parameters I_{Ph}, I_{rs1}, I_{rs2}, I_{rs3}, R_S, R_{Sh}, a_1, a_2, and a_3 (0.498A, 0.293μA, 0.247μA, 0.239μA, 0.0143Ω, 74.198Ω, 1.94, 1.99, 1.99), and (0.292A, 0.194μA, 0.175μA, 0.112μA, 0.007Ω, 44.101Ω, 1.92, 1.94, and 1.95). According to Table 7, the suggested ESM technique has the shortest computation time, 277 seconds, when compared to those other existing techniques like ABSO (392 seconds), GA (374 seconds), CM (358 seconds), ABC (328 seconds), and APSO (293 sec).

Table 4 Estimated model parameters for DDM of (SPR-P5-250UPP) Polycrystalline solar cell.

Algorithm	I_{Ph} (A)	I_{rs1} (μA)	I_{rs2} (μA)	R_S (Ω)	R_{sh}(Ω)	a_1	a_2	Time (S)
ABSO	0.764	0.44785	0.5495	0.0579	84.572	1.34	1.59	429
GA	0.760	0.39752	0.5274	0.0524	96.329	1.31	1.68	416
CM	0.765	0.38183	0.5579	0.0537	98.914	1.36	1.72	388
ABC	0.763	0.39529	0.5816	0.0542	76.482	1.42	1.83	363
APSO	0.761	0.37494	0.5464	0.0563	72.752	1.4	1.71	357
Proposed ESM	0.76	0.33197	0.5372	0.0521	64.235	1.38	1.62	324

Table 5 Estimated model parameters for DDM of (STP250S) polycrystalline solar cell.

Algorithm	I_{Ph}	I_{rs1} (μA)	I_{rs2} (μA)	R_S (Ω)	R_{sh}(Ω)	a_1	a_2	Time (S)
ABSO	0.621	0.4587	0.4239	0.0287	64.572	1.24	1.49	412
GA	0.653	0.3973	0.4274	0.0281	86.153	1.31	1.38	404
CM	0.689	0.38274	0.4195	0.0275	76.176	1.26	1.42	398
ABC	0.632	0.36529	0.4104	0.0289	72.753	1.32	1.33	373
APSO	0.592	0.34947	0.4009	0.0295	69.637	1.24	1.32	347
Proposed ESM	0.586	0.31196	0.3974	0.0277	61.715	1.21	1.32	317

Table 6 Estimated model parameters for TDM of (SPR-P5-250UPP) Polycrystalline solar cell.

Algorithm	I_{Ph}	I_{rs1} (μA)	I_{rs2} (μA)	I_{rs3}(μA)	R_S (Ω)	R_{sh}(Ω)	a_1	a_2	a_3	Time (S)
ABSO	0.498	0.293	0.247	0.239	0.0143	74.198	1.94	1.99	1.99	402
GA	0.487	0.275	0.239	0.224	0.0132	77.378	1.91	1.98	1.97	384
CM	0.476	0.259	0.228	0.195	0.0121	66.276	1.96	1.92	1.94	368
ABC	0.463	0.261	0.220	0.174	0.0111	62.653	1.92	1.93	1.98	343
APSO	0.457	0.249	0.219	0.169	0.0101	59.697	1.94	1.92	1.95	327
Proposed SM	0.422	0.227	0.211	0.154	0.0099	51.115	1.91	1.92	1.91	297

Table 7 Estimated model parameters for TDM of (STP250S) Monocrystalline solar cell.

Algorithm	I_{Ph}	I_{rs1} (µA)	I_{rs2} (µA)	I_{rs3}(µA)	R_S (Ω)	R_{sh}(Ω)	a_1	a_2	a_3	Time (S)
ABSO	0.398	0.273	0.232	0.212	0.0128	94.218	1.95	1.99	1.99	392
GA	0.377	0.255	0.213	0.202	0.0113	67.548	1.92	1.98	1.99	374
CM	0.366	0.231	0.206	0.187	0.0102	58.226	1.94	1.96	1.97	358
ABC	0.343	0.216	0.198	0.152	0.0094	47.123	1.93	1.94	1.96	328
APSO	0.317	0.201	0.184	0.137	0.0082	45.547	1.95	1.96	1.97	293
Proposed SM	0.292	0.194	0.175	0.112	0.0074	44.101	1.92	1.94	1.95	277

4.2. ESM for MPPT tracking

The simulation results for the Enhanced Slime Mold MPPT (ESM-MPPT) technique and the ABC-based PSO MPPT technique were compared for their performance under normal and partial shading conditions. The performance was measured in terms of the output power of the PV system. Under normal conditions, in monocrystalline solar arrays the ESM-MPPT technique produced an average output power of 5 kW, while the ABC-based PSO MPPT technique produced an average output power of 4.95 kW. Figure 13(a) shows that the ESM-MPPT technique was able to produce 1% higher output power compared to the ABC-based PSO MPPT technique under normal conditions. In polycrystalline solar arrays, the ESM-MPPT technique produced an average output power of 4.95 kW, while the ABC-based PSO MPPT technique produced an average output power of 4.9 kW. Figure 13 (c) shows that the ESM-MPPT technique was able to produce 5% higher output power compared to the ABC-based PSO MPPT technique under normal conditions. Under partial shading conditions, we have taken irradiance range from 1000 w/m2 to 100w/m2.

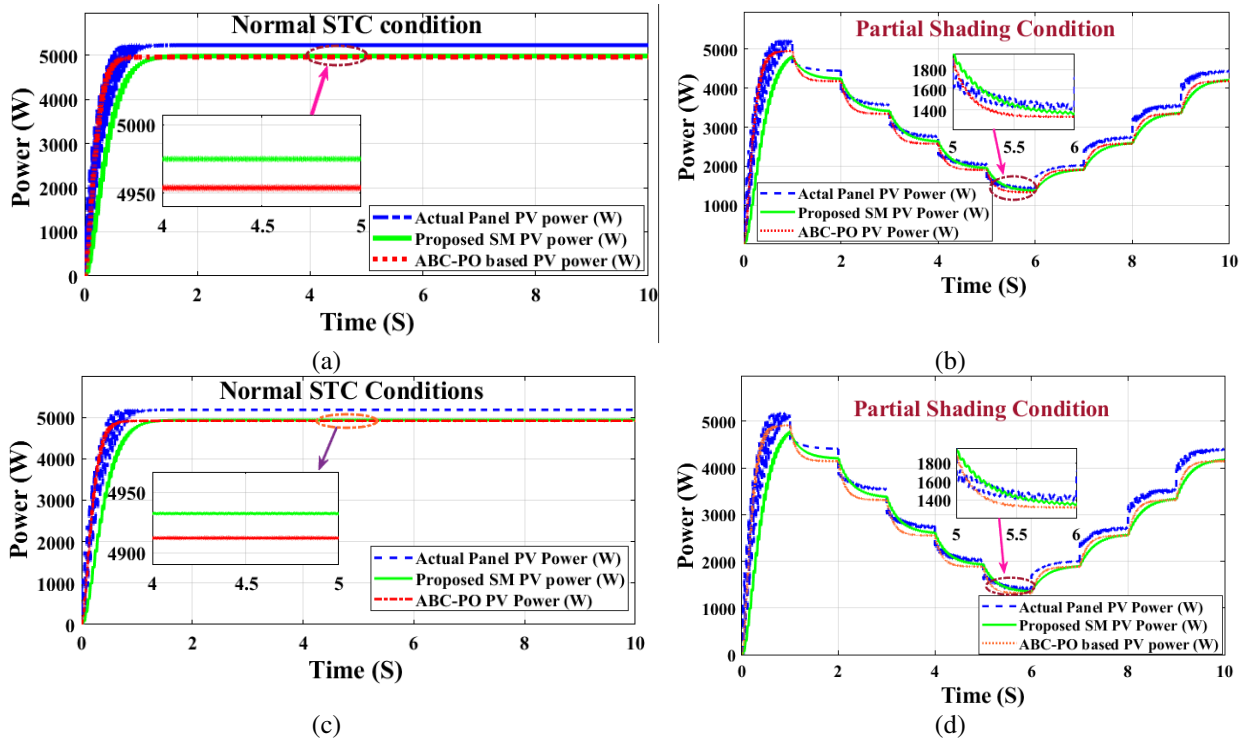

Fig. 13 Maximum Output power of (a) Monocrystalline under Normal STC, (b) Monocrystalline under PSC and (c) Polycrystalline under Normal STC, (d) Polycrystalline under PSC.

Both in monocrystalline and polycrystalline solar arrays, the ESM-MPPT technique produced better output power compared to the ABC-based PSO MPPT technique. Figures 13(b) and 13(d) show that the ESM-MPPT technique was able to produce higher output power at each irradiance condition compared to the ABC-based PSO MPPT technique even under the least irradiance level that we have considered. To investigate the computational efficiency of proposed ESM technique has less amount of absolute error for Mono Crystalline, Poly Crystalline solar panels. The absolute error values for various existing algorithms such as ABSO, GA, CM, ABC, and APSO are shown in Fig. 14 (a)-(f). From figure, it is confirmed that proposed ESM technique has faster convergence, and lower RMSE content.

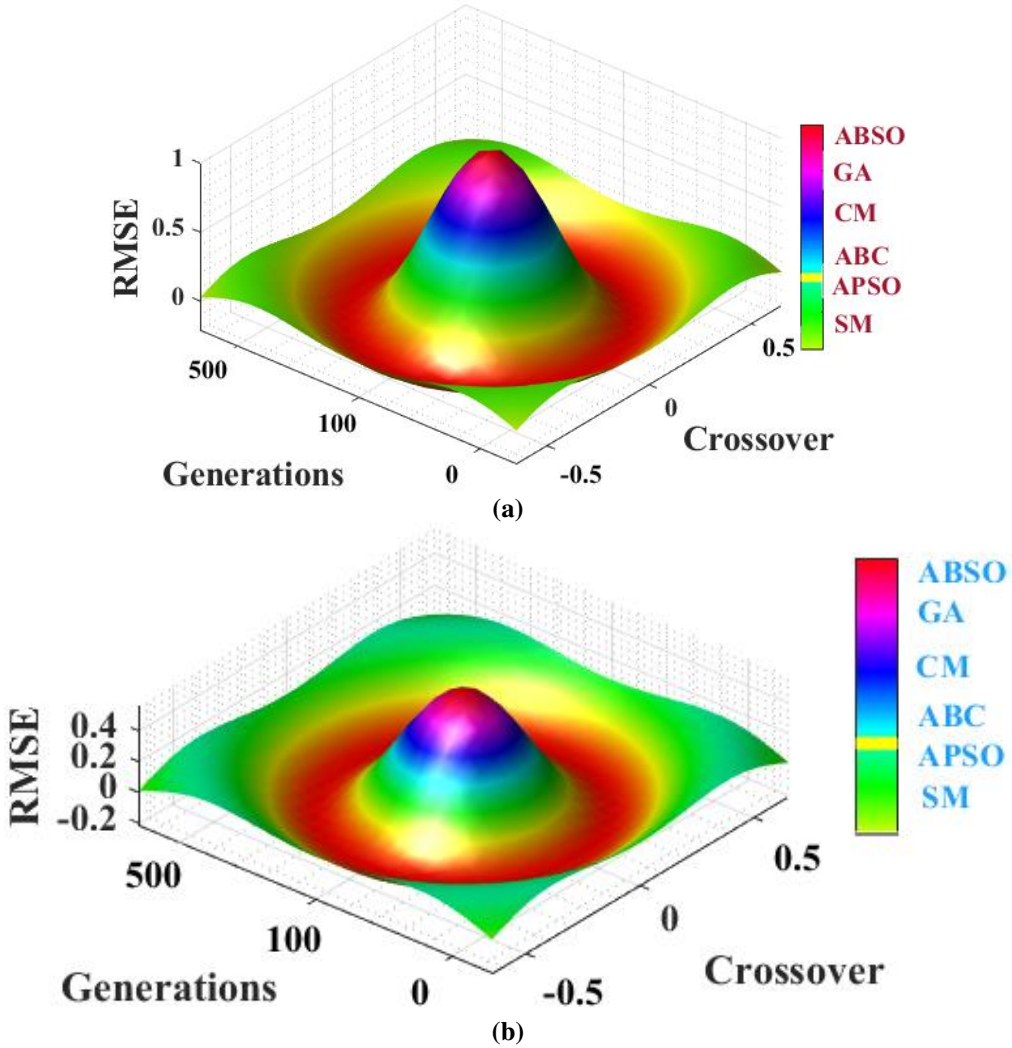

Fig.14 Comparison of RMSE behaviour for Proposed ESM and existing algorithms.

5. Conclusion

Eliminating unknown parameters is crucial for accurately maintaining the maximum power point of a solar panel. This paper suggests utilizing an Enhanced Slime Mold (ESM) optimization algorithm to tackle these challenges. It is essential to eliminate the unknown parameters in solar panel and maintains maximum power accurately. This paper presents the Enhanced Slime Mold (ESM) optimization algorithm to resolve the above-mentioned issues. Model the solar panel and its parasitic parameters as an optimization problem, with the objective of maximizing the power output of the panel under partial shading conditions. Apply the SMO algorithm to the optimization problem, where the algorithm simulates the behavior of slime molds to search for the optimal solution. During the optimization process, the algorithm adjusts the parasitic parameters to reduce the impact of partial shading and maximize the power output of the panel. Once the optimization process is complete, the extracted parasitic parameters can be used to design more efficient solar panels that are less affected by partial shading. Overall, the ESM algorithm can efficiently search for optimal solutions in complex optimization problems, such as the extraction of parasitic parameters and reduction of partial shading effects in solar panels. To evaluate the performance of proposed ESM algorithm in determining model parameters for SPR-P5-250UPP polycrystalline modules, as well as STP250S monocrystalline modules. The results indicate that ESM algorithm can achieve optimal identification results with the least computational effort compared to other existing algorithms, such as ABSO, GA, CM, ABC, and APSO.

References

[1] IEA (2020), World Energy Outlook 2020, IEA, Paris https://www.iea.org/reports/world-energy-outlook-2020, License: CC BY 4.0.

[2] IEA (2021), World Energy Outlook 2021, IEA, Paris https://www.iea.org/reports/world-energy-outlook-2021, License: CC BY 4.0.

[3] IEA (2022), World Energy Outlook 2022, IEA, Paris https://www.iea.org/reports/world-energy-outlook-2022, License: CC BY 4.0 (report); CC BY NC SA 4.0.

[4] REN21 Renewables 2022 Global Status Report, https://www.ren21.net/reports/global-status-report.

[5] T. Okubo, T. Shimizu, K. Hasegawa, Y. Kikuchi, S. Manzhos, and M. Ihara, "Factors affecting the techno-economic and environmental performance of on-grid distributed hydrogen energy storage systems with solar panels," Energy (Oxf.), vol. 269, no. 126736, p. 126736, 2023.

[6] Q. Li, D. Zhang, and K. Yan, "A solar irradiance forecasting framework based on the CEE-WGAN-LSTM model," Sensors (Basel), vol. 23, no. 5, p. 2799, 2023.

[7] V. L. Mishra, Y. K. Chauhan, and K. S. Verma, "A critical review on advanced reconfigured models and metaheuristics based MPPT to address complex shadings of solar array," Energy Convers. Manag., vol. 269, no. 116099, p. 116099, 2022.

[8] S. Motahhir, A. El Hammoumi, and A. El Ghzizal, "The most used MPPT algorithms: Review and the suitable low-cost embedded board for each algorithm," J. Clean. Prod., vol. 246, no. 118983, p. 118983, 2020.

[9] A. Mohapatra, B. Nayak, P. Das, and K. B. Mohanty, "A review on MPPT techniques of PV system under partial shading condition," Renew. Sustain. Energy Rev., vol. 80, pp. 854–867, 2017.

[10] J. Dang, G. Wang, C. Xia, R. Jia, and P. Li, "Research on the parameter identification of PV module based on fuzzy adaptive differential evolution algorithm," Energy Rep., vol. 8, pp. 12081–12091, 2022.

[11] A. A. Z. Diab, H. M. Sultan, T. D. Do, O. M. Kamel, and M. A. Mossa, "Coyote optimization algorithm for parameters estimation of various models of solar cells and PV modules," IEEE Access, vol. 8, pp. 111102–111140, 2020.

[12] S. Arandhakar, N. Chaudhary, S. R. Depuru, R. K. Dubey, and M. N. Bhukya, "Analysis and implementation of robust metaheuristic algorithm to extract essential parameters of solar cell," IEEE Access, vol. 10, pp. 40079–40092, 2022.

[13] H. M. Ridha, A. A. Heidari, M. Wang, and H. Chen, "Boosted mutation-based Harris hawks optimizer for parameters identification of single-diode solar cell models," Energy Convers. Manag., vol. 209, no. 112660, p. 112660, 2020.

[14] A. Abbassi, R. Ben Mehrez, B. Touaiti, L. Abualigah, and E. Touti, "Parameterization of photovoltaic solar cell double-diode model based on improved arithmetic optimization algorithm," Optik (Stuttg.), vol. 253, no. 168600, p. 168600, 2022.

[15] A. A. Z. Diab, H. M. Sultan, R. Aljendy, A. S. Al-Sumaiti, M. Shoyama, and Z. M. Ali, “Tree growth based optimization algorithm for parameter extraction of different models of photovoltaic cells and modules,” IEEE Access, vol. 8, pp. 119668–119687, 2020.
[16] F. Perin Gasparin, F. Detzel Kipper, F. Schuck de Oliveira, and A. Krenzinger, “Assessment on the variation of temperature coefficients of photovoltaic modules with solar irradiance,” Sol. Energy, vol. 244, pp. 126–133, 2022.
[17] Suman, P. Sharma, and P. Goyal, “Analysing the effects of solar insolation and temperature on PV cell characteristics,” Mater. Today, vol. 45, pp. 5539–5543, 2021.
[18] D. Sharma, M. F. Jalil, M. S. Ansari, and R. C. Bansal, “A review of PV array reconfiguration techniques for maximum power extraction under partial shading conditions,” Optik (Stuttg.), vol. 275, no. 170559, p. 170559, 2023.
[19] C. E. Clement, J. P. Singh, E. Birgersson, Y. Wang, and Y. S. Khoo, “Hotspot development and shading response of shingled PV modules,” Sol. Energy, vol. 207, pp. 729–735, 2020.
[20] Y. Liu, A. A. Heidari, X. Ye, G. Liang, H. Chen, and C. He, “Boosting slime mould algorithm for parameter identification of photovoltaic models,” Energy (Oxf.), vol. 234, no. 121164, p. 121164, 2021.
[21] M. S. Kumar, P. S. Manoharan, and R. Ramachandran, “Modelling and simulation of ANFIS-based MPPT for PV system with modified SEPIC converter,” Int. J. Bus. Intell. Data Min., vol. 15, no. 3, p. 255, 2019.
[22] A. Askarzadeh and A. Rezazadeh, “Artificial bee swarm optimization algorithm for parameters identification of solar cell models,” Appl. Energy, vol. 102, pp. 943–949, 2013.
[23] B. A. Almashary, “Genetic algorithm based diode model parameters extraction,” J. King Saud Univ. - Eng. Sci., vol. 18, no. 2, pp. 249–259, 2006.
[24] O. Mares, M. Paulescu, and V. Badescu, “A simple but accurate procedure for solving the five-parameter model,” Energy Convers. Manag., vol. 105, pp. 139–148, 2015.
[25] S. L. Sabat, S. K. Udgata, and A. Abraham, “Artificial bee colony algorithm for small signal model parameter extraction of MESFET,” Eng. Appl. Artif. Intell., vol. 23, no. 5, pp. 689–694, 2010.
[26] Z. Erdem, “An advanced particle swarm optimization algorithm for MPPTs in PV systems,” Acta Phys. Pol. A., vol. 132, no. 3–II, pp. 1134–1139, 2017.